Dalton Transactions

PAPER

View Article Online
View Journal | View Issue

Cite this: *Dalton Trans.*, 2014, **43**, 2294

Synthesis, crystal structure and lithium ion conduction of $Li_3BP_2O_8$†

Toru Hasegawa and Hisanori Yamane*

Received 16th October 2013,
Accepted 11th November 2013

DOI: 10.1039/c3dt52917g

www.rsc.org/dalton

Single crystals of $Li_3BP_2O_8$ were prepared by heating a mixture of starting materials with a Li : B : P molar ratio of 22 : 11 : 13 at 933 K in air and by cooling at a rate of −10 K h^{-1}. The X-ray diffraction (XRD) reflections of a single crystal were indexed with triclinic cell parameters: a = 5.1888(5) Å, b = 7.4118(7) Å, c = 7.6735(7) Å, α = 101.18(1)°, β = 105.07(1)°, γ = 90.34(1)° (space group $P\bar{1}$ (no. 2)). In the crystal structure of $Li_3BP_2O_8$, BO_4 and PO_4 tetrahedra share O atoms and form one-dimensional $^1_\infty[BP_2O_8]^{3-}$ chains along the c-axis direction. A polycrystalline $Li_3BP_2O_8$ bulk sample was synthesized by the solid state reaction of $Li_4P_2O_7$ and $LiPO_3$ prepared from the starting materials in advance with H_3BO_3 at 923 K. The lithium ion conductivities measured for the polycrystalline sample by the AC impedance and DC methods were 1.5×10^{-5} S cm^{-1} at 583 K and 6.0×10^{-8} S cm^{-1} at 423 K, respectively.

Introduction

Borophosphates, containing complex anionic groups built of BO_4 and/or BO_3 and PO_4, have been studied due to their rich structural chemistry and potential applications. The structural chemistry of borophosphate anions extends from isolated species, oligomers, rings and chains to layers and frameworks.[1–3] A concept for the classification of crystalline borophosphates in terms of structural chemistry has been proposed by Gurbanova *et al.*[2] and Ewald *et al.*[3] Most borophosphates have been synthesized under hydrothermal conditions, and OH^- and/or H_2O are contained in the structures. Anhydrous borophosphates are rare and usually prepared by high-temperature solid state reaction.[3,4]

Anhydrous alkali metal borophosphates reported in previous studies are $Li_{22}B_{11}P_{13}O_{60}$, $Li_2B_3PO_8$,[5] $Na_5B_2P_3O_{13}$,[6] $Na_3B_6PO_{13}$ and $Na_3BP_2O_8$.[7] $Li_{22}B_{11}P_{13}O_{60}$ and $Li_2B_3PO_8$ were found by X-ray diffraction (XRD) in the study of the Li_2O–B_2O_3–P_2O_5 system.[5] Powder XRD data of these compounds have been reported, but the crystal structures have not been analyzed. $Na_5B_2P_3O_{13}$ was prepared by heating stoichiometric amounts of $NaH_2PO_4{\cdot}H_2O$ and $NaBO_2{\cdot}H_2O$ at 1073 K. Loop-branched chains of $[B_2P_3O_{13}]$ are contained in the structure of $Na_5B_2P_3O_{13}$.[6] $Na_3B_6PO_{13}$ and $Na_3BP_2O_8$, consisting of $^1_\infty[B_6PO_{13}]^{3-}$ chains and $^1_\infty[BP_2O_8]^{3-}$ chains, respectively, were prepared in autoclaves at 553 K using boric acid or sodium dihydrogen phosphate as the flux.[7]

Borates and phosphates are known to be glass forming materials, and formation of borophosphate glass in the Li_2O–B_2O_3–P_2O_5 system was reported by Tien and Hummel.[5] The structure and electrical conductivity of lithium borophosphate glasses with the composition of $50Li_2O$–xB_2O_3–$(1-x)P_2O_5$ (x = 2–25 mol%) was investigated,[8] and a lithium ion conductivity of 1.6×10^{-7} S cm^{-1} at room temperature was measured for a glass of $0.45Li_2O$–$0.275B_2O_3$–$0.275P_2O_5$ composition.[9]

In the present study, the crystalline phase of $Li_3BP_2O_8$ was synthesized in the Li_2O–B_2O_3–P_2O_5 system. The crystal structure of $Li_3BP_2O_8$ was determined by single crystal X-ray diffraction (XRD), and the electrical properties were characterized for polycrystalline bulk samples.

Experimental

H_3BO_3 (99.5%, Wako Pure Chemical Ind.), Li_2CO_3 (99.0%, Wako Pure Chemical Ind.) and $NH_4H_2PO_4$ (99.0%, Wako Pure Chemical Ind.) were used as starting powders. To prepare $Li_{22}B_{11}P_{13}O_{60}$ reported in the previous study,[5] the starting powders were weighed with a molar ratio of Li : B : P = 22 : 11 : 13, mixed in an agate mortar with a pestle and pressed into a pellet. The pellet was placed on a platinum plate and heated at 473 K for 9 h in air with an electric furnace. After cooling, the product was powdered, pelletized and heated at 823 K for 12 h. The crystalline phases in the obtained sample were identified by powder XRD using CuKα radiation with a graphite monochromator mounted on a powder diffractometer (Rigaku, Model RINT2000).

Institute of Multidisciplinary Research for Advanced Materials, Tohoku University, 2-1-1 Katahira, Aoba-ku, Sendai 980-8577, Japan. E-mail: yamane@tagen.tohoku.ac.jp; Fax: +81 22 217 5813

†CCDC 966781. For crystallographic data in CIF or other electronic format see DOI: 10.1039/c3dt52917g

For the preparation of single crystals, the pellet sample obtained by heating at 823 K was heated again at 933 K for 1 h, cooled to 873 K for 6 h and then cooled to room temperature in the furnace. The product was crushed and a single crystal for crystal structure analysis was picked up, fixed to the tip of a glass fiber with epoxy resin and set to a goniometer of a single-crystal X-ray diffractometer (Rigaku, R-AXIS RAPID-II). X-ray diffraction data of the single crystal were collected using Mo*K*α radiation with a graphite monochromator and an imaging plate. Unit cell refinement and absorption collection were performed by the programs PROCESS-AUTO[10] and NUMABS,[11] respectively. The crystal structure was solved by direct methods using the SIR2004 program[12] and structure parameters were refined by full-matrix least-squares on F^2 using the SHELXL-97 program.[13] Crystal structure illustration and Madelung energy calculation were carried out using the VESTA program.[14]

Polycrystalline $Li_3BP_2O_8$ samples for electrical conductivity measurement were synthesized with a mixture of $Li_4P_2O_7$ and $LiPO_3$ powders prepared in advance and H_3BO_3 powder. A powder mixture of Li_2CO_3 and $NH_4H_2PO_4$ with a molar ratio of Li : P = 2 : 1 was calcined at 473 K for 9 h. $Li_4P_2O_7$ was synthesized by heating the calcined mixture at 823 K for 12 h. For the synthesis of $LiPO_3$, a mixture of Li_2CO_3 and $NH_4H_2PO_4$ with a molar ratio of Li : P = 1 : 1 was calcined at 423 K for 12 h. The calcined powder was ground and heated again at 473 K for 12 h, and then heated at 823 K for 12 h.

The powders of $Li_4P_2O_7$, $LiPO_3$ and H_3BO_3 weighed with a molar ratio of Li : B : P = 3 : 1 : 2 were mixed, pressed into pellets, and heated on a Pt plate two times at 923 K for 12 h with intermediate pulverization and pelletization. The obtained polycrystalline samples were powdered and the crystalline phases in the samples were analyzed by powder XRD. Rietveld analysis of the powder XRD pattern was performed using the RIETAN-FP program.[15] Chemical analysis of the polycrystalline sample was carried out using an inductively coupled plasma-optical (ICP) emission spectrometer (SPECTRO, SPECTRO ARCOS).

The electrical conductivity of the polycrystalline sample was measured by the AC impedance method using an impedance analyzer (WAYNE KERR, LCR METER 4100) in a frequency range of 20 Hz–1 MHz in a temperature range of 473–583 K. Graphite or Ag paste was used as the electrode. The electromotive force of a cell Li|$Li_3BP_2O_8$|C was measured with a galvanostat (HOKUTO DENKO, POTENTIOSTAT/GALVANOSTAT HAB-151). Two-probe DC electrical conductivity measurement using Li or C as the electrode was carried out using a digital multimeter.

Results and discussion

Fig. 1(a) shows the powder XRD pattern of the sample prepared by heating a starting mixture of Li_2CO_3, H_3BO_3 and $NH_4H_2PO_4$ with a molar ratio of Li : B : P = 22 : 11 : 13 at 473 K for 9 h, followed by powdering, pelletizing and heating at 823 K for 12 h. Besides the XRD reflections of $Li_{22}B_{11}P_{13}O_{60}$ reported by Tien and Hummel,[5] reflections of Li_3PO_4 and H_3BO_3 were observed. H_3BO_3 was probably formed by the reaction of B_2O_3 with moisture in the air. This polycrystalline

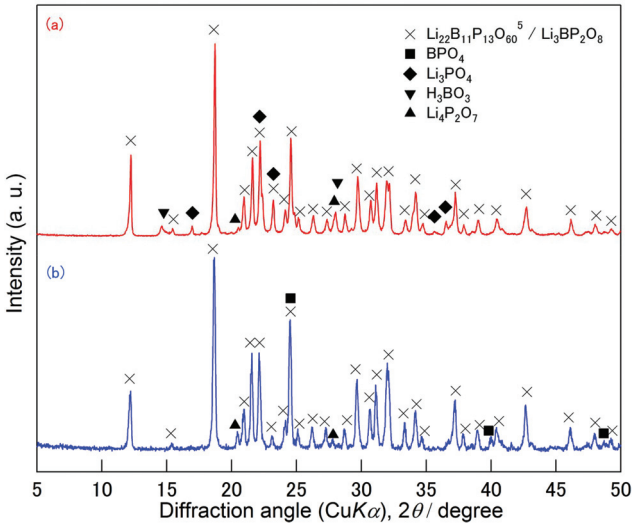

Fig. 1 Powder XRD patterns of samples prepared by heating starting-powder mixtures with a molar ratio of Li : B : P = 22 : 11 : 13 at 823 K for 12 h (a) and such mixtures with a molar ratio of Li : B : P = 2 : 3 : 1 at 923 K for 12 h (b).

Table 1 Crystal data and refinement results for $Li_3BP_2O_8$ [a]

Chemical formula	$Li_3BP_2O_8$
Formula weight, M_r	221.57 g mol^{-1}
Temperature, T	293(2) K
Crystal system	Triclinic
Space group	$P\bar{1}$ (no. 2)
Unit cell dimensions	a = 5.1888(5) Å, α = 101.18(1)°
	b = 7.4118(7) Å, β = 105.07(1)°
	c = 7.6735(7) Å, γ = 90.34(1)°
Unit cell volume, V	279.06(5) Å^3
Z	2
Calculated density, D_{cal}	2.637 Mg m^{-3}
Radiation wavelength, λ	0.71075 Å (MoKα)
Crystal form, color	Colorless
Absorption correction	Numerical
Absorption coefficient, μ	0.784 mm^{-1}
Crystal size	0.176 × 0.168 × 0.072 mm^3
Limiting indices	$-6 \le h \le 6$
	$-9 \le k \le 9$
	$-9 \le l \le 9$
F_{000}	216
θ range for data collection	3.545°–27.49°
Reflections collected/unique	1265/1067
R_{int}	0.0272
Data/restraints/parameters	1265/0/127
Weight parameters, a, b	0.0304, 0.5296
Goodness-of-fit on F^2, S	1.063
$R1$, w$R2$ ($I > 2\sigma(I)$)	0.0329, 0.0748
$R1$, w$R2$ (all data)	0.0407, 0.0809
Largest diff. peak and hole, $\Delta\rho$	0.560, −0.543 e Å^{-3}

[a] $R_1 = \sum||F_o| - |F_c||/\sum|F_o|$. w$R_2 = [\sum w(F_o^2 - F_c^2)^2/\sum(wF_o^2)^2]^{1/2}$, $w = 1/[\sigma^2(F_o^2) + (aP)^2 + bP]$, where F_o is the observed structure factor, F_c is the calculated structure factor, σ is the standard deviation of F_c^2, and $P = (F_o^2 + 2F_c^2)/3$. $S = [\sum w(F_o^2 - F_c^2)^2/(n - p)]^{1/2}$, where n is the number of reflections and p is the total number of parameters refined.

multi-phase sample changed to a colorless transparent glass phase on heating at 973 K. Crystalline phases could not be obtained by slow cooling of the glass phase from 973 K. The multi-phase crystalline sample obtained at 823 K was annealed at 873 K for 100 h, but no grain growth or a change in the combination of the crystalline phases was observed. However, by heating the multi-phase sample at 933 K, grain growth in partial melt conditions was recognized. Single crystals with a size of about 0.2 mm were obtained by cooling from 933 K to 873 K at a rate of −10 K h^{-1}.

The XRD reflections of a single crystal were indexed with triclinic unit-cell parameters of a = 5.1888(5) Å, b = 7.4118(7) Å, c = 7.6735(7) Å, α = 101.18(1)°, β = 105.07(1)°, γ = 90.34(1)°. Considering the cell volume of 279.06(5) $Å^3$, the element numbers in the unit cell were postulated to be $Li_6B_3P_3O_{15}$, which is about 1/4 of $Li_{22}B_{11}P_{13}O_{60}$, for the calculation to solve the crystal structure with the space group using the SIR2004 program. An obtained structure model was improved by relabeling some atoms and by searching missing atoms from the results of differential Fourier synthesis using the SHELXL-97 program. The structural chemical formula of the single crystal was finally determined to be $Li_3BP_2O_8$ (Z = 2) by refinement with an R_1-value (all data) of 4.07% (Table 1). The atomic coordinates, anisotropic displacement parameters and selected bond lengths of $Li_3BP_2O_8$ are listed in Tables 2–4.

Fig. 2 shows the coordination environment of $Li_3BP_2O_8$ using the refined structural parameters. Four O atoms coordinate to the B1 atom and form a boron-centered tetrahedron [BO_4]. The B1–O distances vary from 1.455(3) to 1.484(3) Å. P atoms at P1 and P2 sites are coordinated by four O atoms and in the oxygen tetrahedra [PO_4] with P1–O distances 1.4995(19)–1.5786(18) Å, and P2–O distances 1.4957(19)–1.5717(18) Å. O–B1–O, O–P1–O and O–P2–O angles are in the ranges 105.0–111.4°, 103.6–114.3° and 106.2–112.4°, respectively. The Li1 atom is coordinated by five O atoms. Four of the Li1–O distances range from 1.970(6) to 2.180(6) Å and the Li1–O5 distance is 2.609(6) Å. Li2 and Li3 atoms are at the 4-fold coordination sites with Li2–O and Li3–O distances of 1.876(5)–1.965(5) Å and 1.890(6)–2.213(9) Å, respectively. The bond valence sums for the atoms at the sites of B1, P1, P2, Li1, Li2 and Li3, calculated with the bond lengths and the bond valence parameters presented by Brece and O'Keeffe,[16] were 3.05, 4.97, 5.00, 0.82, 1.15 and 0.91, respectively (Table 4). These values are comparable with the valences of the elements.

The value of the Madelung energy for $Li_3BP_2O_8$ calculated with the structure parameters was −60 600 kJ mol^{-1}, which

Table 2 Atomic coordinates and equivalent isotropic displacement parameters (U_{eq}) for $Li_3BP_2O_8$

Atom	Site	Occ.	x	y	z	U_{eq} [a]/Å^2
Li1	2i	1	0.7757(12)	0.1333(8)	0.3078(8)	0.0311(12)
Li2	2i	1	0.6698(9)	0.4796(7)	0.1455(6)	0.0193(10)
Li3	2i	1	0.1387(11)	0.5327(9)	0.3879(10)	0.0468(18)
B1	2i	1	0.2584(5)	0.9615(4)	0.2316(4)	0.0108(6)
P1	2i	1	0.37120(12)	0.21492(9)	0.55001(9)	0.01021(18)
P2	2i	1	0.11689(12)	0.25094(9)	0.05505(9)	0.01017(18)
O1	2i	1	0.0529(3)	0.8131(3)	0.1482(2)	0.0137(4)
O2	2i	1	0.4736(3)	0.1125(2)	0.7151(2)	0.0127(4)
O3	2i	1	0.9397(4)	0.3047(3)	0.1836(2)	0.0152(4)
O4	2i	1	0.2023(3)	0.3680(2)	0.6055(2)	0.0135(4)
O5	2i	1	0.2817(3)	0.0826(2)	0.1061(2)	0.0129(4)
O6	2i	1	0.3045(4)	0.4066(3)	0.0591(3)	0.0169(4)
O7	2i	1	0.1831(3)	0.0641(2)	0.3957(2)	0.0113(4)
O8	2i	1	0.6000(3)	0.2751(3)	0.4847(2)	0.0145(4)

[a] $U_{eq} = (\sum_i \sum_j U_{ij}\, a_i^* a_j^*\, \boldsymbol{a}_i \cdot \boldsymbol{a}_j)/3$.

Table 3 Anisotropic displacement parameters (U_{ij}/Å) for $Li_3BP_2O_8$

Atom	Site	U_{11}	U_{22}	U_{33}	U_{23}	U_{13}	U_{12}
Li1	2i	0.037(3)	0.025(3)	0.039(3)	0.006(2)	0.025(3)	0.003(2)
Li2	2i	0.015(2)	0.025(3)	0.015(2)	0.0024(19)	0.0006(18)	0.0041(18)
Li3	2i	0.020(3)	0.037(4)	0.066(5)	−0.022(3)	0.004(3)	−0.001(2)
B1	2i	0.0093(13)	0.0124(14)	0.0094(13)	0.0008(11)	0.0015(11)	−0.0001(10)
P1	2i	0.0099(3)	0.0101(3)	0.0104(3)	0.0012(2)	0.0030(2)	0.0019(2)
P2	2i	0.0106(3)	0.0096(3)	0.0102(3)	0.0018(2)	0.0028(2)	0.0010(2)
O1	2i	0.0146(9)	0.0147(10)	0.0106(9)	0.0013(7)	0.0022(7)	−0.0037(7)
O2	2i	0.0119(8)	0.0142(9)	0.0132(9)	0.0034(7)	0.0046(7)	0.0043(7)
O3	2i	0.0167(9)	0.0166(10)	0.0142(9)	0.0033(8)	0.0071(8)	0.0059(7)
O4	2i	0.0135(9)	0.0119(9)	0.0148(9)	0.0010(7)	0.0041(7)	0.0035(7)
O5	2i	0.0146(9)	0.0126(9)	0.0147(9)	0.0060(7)	0.0073(7)	0.0045(7)
O6	2i	0.0156(9)	0.0138(10)	0.0197(10)	0.0058(8)	0.0004(8)	−0.0030(7)
O7	2i	0.0112(8)	0.0119(9)	0.0109(9)	0.0004(7)	0.0044(7)	0.0003(7)
O8	2i	0.0129(9)	0.0150(10)	0.0149(9)	0.0004(7)	0.0046(7)	−0.0004(7)

Table 4 Selected bond lengths and bond valence sums (V_i), for $Li_3BP_2O_8$ [a]

Li1–O8	1.970(6)	B1–O1	1.455(3)
Li1–O3	2.031(6)	B1–O5^{vii}	1.463(3)
Li1–O7^{i}	2.143(6)	B1–O2^{iv}	1.484(3)
Li1–O2^{ii}	2.180(6)	B1–O7^{vii}	1.484(3)
Li1–O5	2.609(6)	V_B	3.05
V_{Li1}	0.82		
Li2–O6	1.876(5)	P1–O8	1.4995(19)
Li2–O3	1.919(5)	P1–O4	1.5018(18)
Li2–O6^{iii}	1.953(5)	P1–O7	1.5742(18)
Li2–O4^{iv}	1.965(5)	P1–O2	1.5786(18)
V_{Li2}	1.15	V_{P1}	4.97
Li3–O8^{iv}	1.890(6)	P2–O6	1.4957(19)
Li3–O4^{v}	1.930(6)	P2–O3^{vi}	1.5164(19)
Li3–O3^{vi}	2.119(6)	P2–O1^{viii}	1.5578(18)
Li3–O4	2.213(9)	P2–O5	1.5717(18)
V_{Li3}	0.91	V_{P2}	5.00

[a] Symmetry codes: (i) $x + 1, y, z$; (ii) $-x + 1, -y, -z + 1$; (iii) $-x + 1, -y + 1, -z$; (iv) $-x + 1, -y + 1, -z + 1$; (v) $-x, -y + 1, -z + 1$; (vi) $x - 1, y, z$; (vii) $x, y + 1, z$; (viii) $-x, -y + 1, -z$. Bond valence parameters: Li^+: 1.466 Å, B^{3+}: 1.371 Å, P^{5+}: 1.617 Å.[16]

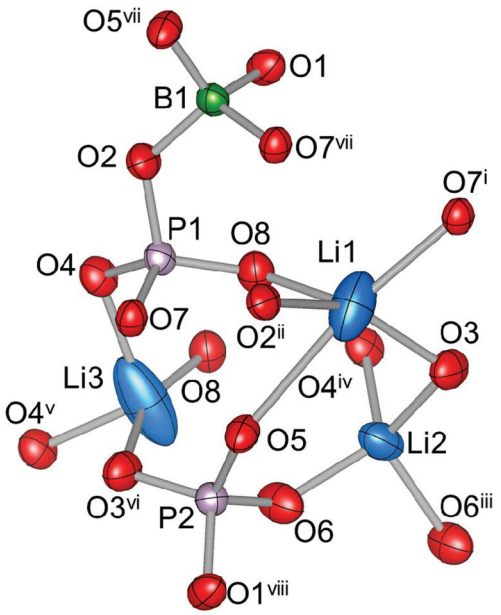

Fig. 2 Atomic arrangement around Li, B, P and O atoms in the structure of $Li_3BP_2O_8$. Displacement ellipsoids are drawn at the 90% probability level. Symmetry codes: (i) $x + 1, y, z$; (ii) $-x + 1, -y, -z + 1$; (iii) $-x + 1, -y + 1, -z$; (iv) $-x + 1, -y + 1, -z + 1$; (v) $-x, -y + 1, -z + 1$; (vi) $x - 1, y, z$; (vii) $x, y + 1, z$; (viii) $-x, -y + 1, -z$.

was almost identical to the value of −59 900 kJ mol^{-1} (difference Δ = 1.1%) of the Madelung energies: Li_2O −3500 kJ mol^{-1},[17] B_2O_3 −2190 kJ mol^{-1} [18] and P_2O_5 −43 700 kJ mol^{-1} [19] with the formula $Li_3BP_2O_8 = 3/2Li_2O + 1/2B_2O_3 + P_2O_5$.

As shown in Fig. 3(a), all oxygen atoms of the BO_4 tetrahedron are shared by four PO_4 tetrahedra. One-dimensional $^1_\infty[BP_2O_8]^{3-}$ chains are formed in the *c*-axis direction by linking the four-membered rings composed of two PO_4 and two BO_4 tetrahedra. The fundamental building unit (FBU) can be expressed by the description of Ewald *et al.* as 6□ : □<4□>□.[3] Similar $^1_\infty[BP_2O_8]^{3-}$ chains have been reported in the crystal structures of $Na_3BP_2O_8$ (space group $C2/c$)[7] and $RbZnBP_2O_8$ (space group $P\bar{1}$).[20]

Li1 sites are in the layers of $^1_\infty[BP_2O_8]^{3-}$ chains, and Li2 and Li3 sites align on the *a*–*c* plane at y = 0.41–0.59 (Fig. 3(b)), forming zigzag chains along the $a + c$ direction (Fig. 3(c)). The distances of Li2–Li2, Li2–Li3 and Li3–Li3 are in the range 2.531(5)–2.624(7) Å (Fig. 3(c)). The Li–Li distances between the zigzag chains are 3.688(7)–4.588(6) Å. The relatively short Li–Li interatomic distances in the chains may suggest a lithium ion conduction path of $Li_3BP_2O_8$.

In order to reveal Li ion conduction, preparation of $Li_3BP_2O_8$ bulk samples was attempted. Fig. 1(b) shows the powder XRD pattern of the sample prepared by heating the starting powders of H_3BO_3, Li_2CO_3 and $NH_4H_2PO_4$ with a Li : B : P molar ratio of 3 : 1 : 2 at 473 K for 9 h, followed by grinding, pelletizing and heating two times at 923 K for 12 h with intermediate pulverization and pelletization. In this powder XRD pattern, the reflection peaks of BPO_4 and $Li_4P_2O_7$ were seen besides the peaks of $Li_3BP_2O_8$ indexed with the lattice parameters determined by the single crystal XRD analysis. BPO_4 is a stable compound with a melting point of about 1673 K. Once BPO_4 was crystallized in the sample, it was difficult to react BPO_4 completely with $Li_4P_2O_7$. The single phase of $Li_3BP_2O_8$ was prepared from $Li_4P_2O_7$ (m.p.: 1149 K), $LiPO_3$ (m.p.: 929 K) and H_3BO_3 (decomposed to B_2O_3 at 458 K, m.p. of B_2O_3: 753 K) as starting materials.

Fig. 4 shows the result of Rietveld refinement for the powder XRD pattern of the $Li_3BP_2O_8$ sample using the crystal structure model presented by the single crystal XRD. All peaks were indexed with the lattice parameters refined by the Rietveld analysis: a = 5.18971(18) Å, b = 7.41030(26) Å, c = 7.67204(29) Å, α = 101.14(1)°, β = 105.05(1)° and γ = 90.34(1)°, which agreed with those of single crystal XRD (Table 1). The final *R*-factors defined in ref. 21 were R_{wp} = 0.112, R_p = 0.083, R_B = 0.030, R_F = 0.017 and S = 2.243. As listed in Table 5, the *d* values and intensities of the XRD peaks reported for $Li_{22}B_{11}P_{13}O_{60}$ by Tien and Hummel[5] are comparable to the data for $L_3BP_2O_8$ revealed in the present study. The polycrystalline bulk sample of $Li_3BP_2O_8$ was dissolved in an HCl water solution, and the contents of Li_2O, B_2O_3 and P_2O_5 analyzed by ICP spectrometry were 19.4, 15.7 and 62.4 mass% (total 97.5%), respectively, which were fairly consistent with the ideal compositions (Li_2O: 20.2%, B_2O_3: 15.7%, P_2O_5: 64.1%).

The electrical conductivity was measured by the AC impedance method with the electrodes of graphite or Ag paste coated on both sides of the sample disk. The relative density of the polycrystalline $Li_3BP_2O_8$ bulk sample disk (diameter: 6.01 mm, thickness: 1.02 mm) was approximately 74%. Fig. 5 shows plots of the impedance measured at 453, 513, 553 and 583 K. The semicircles of the impedance plots could not be separated into intra-grain and grain-boundary parts. The total resistances of the $Li_3BP_2O_8$ polycrystalline bulk sample measured at 453, 513, 553 and 583 K were 1560, 213, 61 and

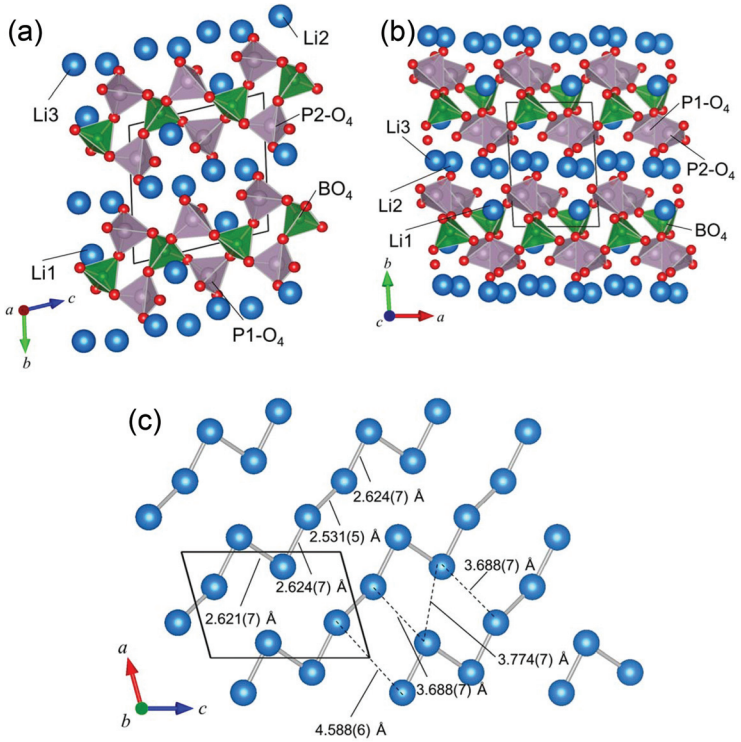

Fig. 3 Projective views of the crystal structure of $Li_3BP_2O_8$ along the *a* axis (a), the *c* axis (b) and the *b* axis (y = 0.41–0.59) (c).

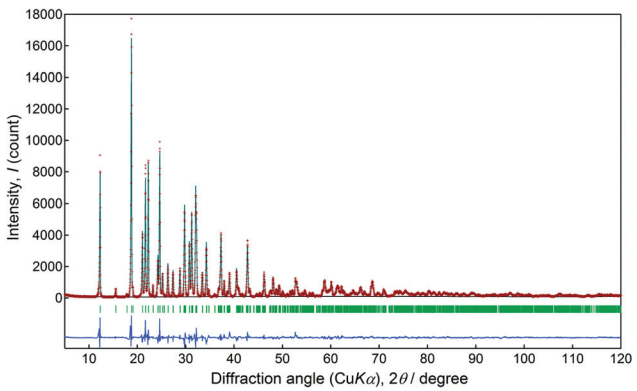

Fig. 4 Observed, calculated and difference XRD profiles for $Li_3BP_2O_8$. The observed data are indicated by dots and the profiles calculated by Rietveld refinement and the differences between the observed and calculated patterns are shown by solid lines. The short vertical lines below the profiles mark the positions of all possible Bragg reflections.

Table 5 XRD data for $Li_{22}B_{11}P_{13}O_{60}$ [5] and $Li_3BP_2O_8$ [a]

$Li_{22}B_{11}P_{13}O_{60}$ [5]		$Li_3BP_2O_8$					
d[Å]	I/I_0	h	k	l	d_{cal}	I_{obs}	I_{cal}
7.25	75	1	0	1	7.258	45	43
4.75	100	1	0	−1	4.751	100	100
4.25	22	1	−1	0	4.239	25	26
4.11	44	1	1	−1	4.120	47	47
4.00	41	1	1	0	4.009	53	54
3.83	20	1	−1	−1	3.844	4	4
3.69	19	1	0	1	3.686	16	16
3.63	58	0	2	0	3.629	32	33
3.55	11	0	1	−2	3.544	8	8
3.40	13	1	0	−2	3.398	14	14
3.27	8	1	1	−2	3.269	11	11
3.11	15	1	1	1	3.108	11	12
3.02	41	0	1	2	3.012	34	36
2.92	19	1	−1	−2	2.916	23	24
2.88	25	0	2	−2	2.872	35	37
2.80	44	1	−2	1	2.799	43	45
2.69	10	1	2	−2	2.687	11	11
2.62	25	1	0	2	2.624	15	17
2.59	9	2	0	−1	2.586	2	2
2.42	26	1	2	1	2.415	28	29
2.38	13	2	0	−2	2.376	6	6
2.32	12	2	1	−2	2.310	7	7
2.23	15	0	2	−3	2.231	11	11
2.12	25	2	2	−1	2.116	18	18
1.969	9	1	2	2	1.967	12	12
1.895	10	2	−1	−3	1.896	6	6

[a] Refined lattice parameters of $Li_3BP_2O_8$: a = 5.18971(18) Å, b = 7.41030(26) Å, c = 7.67204(29) Å, α = 101.14(1)°, β = 105.05(1)°, γ = 90.34(1)°.

24 kΩ, respectively, which were converted to electrical conductivities of 2.3×10^{-7}, 1.7×10^{-6}, 5.9×10^{-6} and 1.5×10^{-5} S cm^{-1}, respectively. No difference was observed between the conductivities measured with the graphite electrodes and the Ag paste electrodes.

Fig. 6 shows a logarithmic plot of the electrical conductivities measured by the AC impedance method as a function of reciprocal measurement temperatures. The results of the DC measurement with Li metal electrodes added in the plot

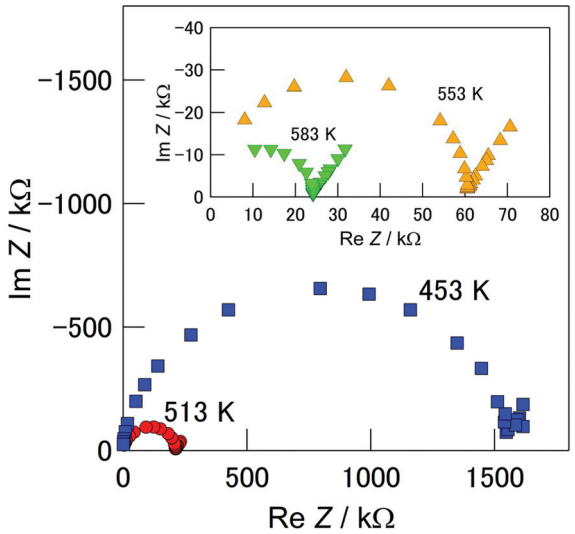

Fig. 5 Complex impedance plots for a polycrystalline $Li_3BP_2O_8$ sample at 453, 513, 553 and 583 K.

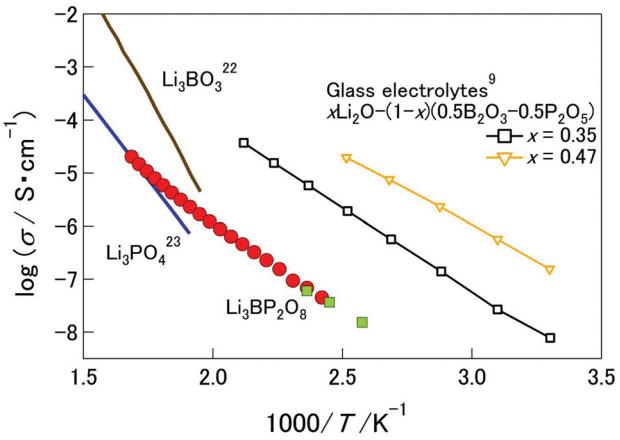

Fig. 6 Arrhenius plots of the conductivities of $Li_3BP_2O_8$ measured by the AC (●) and DC methods with Li metal electrodes (■). The conductivities of $xLi_2O–(1–x)(0.5B_2O_3–0.5P_2O_5)$ glass electrolytes (x = 0.35, 0.47),[9] Li_3BO_3 [22] and Li_3PO_4 [23] are also shown for comparison.

are almost in the same line as that of the AC conductivities. Polarization was observed when the DC conductivity was measured with carbon electrodes, the values being over two orders of magnitude smaller than the conductivities measured with the Li electrodes. An electromotive force of 3.3 V was measured at 343 K for an Li|$Li_3BP_2O_8$|C cell. These results evidenced Li ion conduction with a high transport number close to 1.

Lithium ion conductivities of $xLi_2O–(1–x)(0.5B_2O_3–0.5P_2O_5)$ glass electrolytes (x = 0.35, 0.47),[9] Li_3BO_3 [22] and Li_3PO_4 [23] are also shown in Fig. 6 for comparison. The Li ion conductivity of $Li_3BP_2O_8$ was about two orders of magnitude smaller than the conductivities of the glasses. The activation energy of $Li_3BP_2O_8$ (68 kJ mol^{-1}) was close to the energies of the glasses ($0.35Li_2O–0.325B_2O_3–0.325P_2O_5$: 60 kJ mol^{-1}, $0.47Li_2O–0.265B_2O_3–0.265P_2O_5$: 51 kJ mol^{-1}), and lower than that of Li_3BO_3 (167 kJ mol^{-1}) and Li_3PO_4 (93 kJ mol^{-1}). The Li ion conductivity of $Li_3BP_2O_8$ was larger than the conductivities of Li_3BO_3 and Li_3PO_4 in the low temperature region.

As described by the results of crystal structure analysis, a diffusion path was expected in the a + c-axis direction. $Li_3BP_2O_8$ might exhibit anisotropy of Li ion conduction, and higher conductivities would be expected for a single crystal bulk, or a polycrystalline bulk and a film with preferred orientation.

Summary

Lithium borophosphate, $Li_{22}B_{11}P_{13}O_{60}$, reported in a previous study[5] was revealed to be $Li_3BP_2O_8$ which crystallizes in the triclinic space group $P\bar{1}$ (no. 2). B and P atoms are located at tetrahedral sites of O atoms and form $^1_\infty[BP_2O_8]^{3-}$ chains by sharing the vertex oxygen atoms of the tetrahedra. A polycrystalline bulk sample of single-phase $Li_3BP_2O_8$ was prepared by using a powder mixture of $Li_4P_2O_7$, $LiPO_3$ and H_3BO_3. Li ion conduction of $Li_3BP_2O_8$ was confirmed by AC impedance and DC measurements. The ionic conductivity measured for the polycrystalline $Li_3BP_2O_8$ sample was 1.5 × 10^{-5} S cm^{-1} at 583 K.

References

1 R. Kniep, H. Engelhardt and C. Hauf, *Chem. Mater.*, 1998, **10**, 2930–2934.
2 O. A. Gurbanova and E. L. Belokoneva, *Crystallogr. Rep.*, 2007, **52**, 624–633.
3 B. Ewald, Y.-X. Huang and R. Kniep, *Z. Anorg. Allg. Chem.*, 2007, **633**, 1517–1540.
4 W.-L. Zhang, C.-S. Lin, L. Geng, Y.-Y. Li, H. Zhang, Z.-Z. He and W. D. Cheng, *J. Solid State Chem.*, 2010, **183**, 1108–1113.
5 T. Y. Tien and F. A. Hummel, *J. Am. Ceram. Soc.*, 1961, **44**, 390–394.
6 C. Hauf, T. Friedrich and R. Kniep, *Z. Kristallogr.*, 1995, **210**, 446.
7 D.-B. Xiong, H.-H. Chen, X.-X. Yang and J.-T. Zhao, *J. Solid State Chem.*, 2007, **180**, 233–239.
8 F. Munoz, L. Montagne, L. Pascual and A. Durán, *J. Non-Cryst. Solids*, 2009, **355**, 2571–2577.
9 K. I. Cho, S. H. Lee, K. H. Cho, D. W. Shin and Y. K. Sun, *J. Power Sources*, 2006, **163**, 223–228.
10 *PROCESS-AUTO*. Rigaku/MSC, 9009 New Traila Drive, The Woodlands, TX 77381-5209, USA, and Rigaku, 3-9-12 Akishima, Tokyo 196-8666, Japan. Rigaku/MSC & Rigaku Corporation, 2005.
11 T. Higashi, *NUMABS – Numerical Absorption Correction*, Rigaku Corporation, Tokyo, 1999.

12 M. C. Burla, R. Caliandro, M. Camalli, B. Carrozzini, G. L. Cascarano, L. De Caro, C. Giacovazzo, G. Polidori and R. Spagna, *J. Appl. Crystallogr.*, 2005, **38**, 381–388.
13 G. M. Sheldrick, *Acta Crystallogr., Sect. A: Found. Crystallogr.*, 2008, **64**, 112–122.
14 K. Momma and F. Izumi, *J. Appl. Crystallogr.*, 2008, **41**, 653–658.
15 F. Izumi and K. Momma, *Solid State Phenomena*, 2007, **130**, 15–20.
16 N. E. Brese and M. O'Keeffe, *Acta Crystallogr., Sect. B: Struct. Sci.*, 1991, **47**, 192–197.
17 E. Zintl, A. Harder and B. Dauth, *Z. Elktrochem. Angew. P.*, 1934, **40**, 588–593.
18 G. E. Gurr, P. W. Montgomery, C. D. Knutson and B. T. Gorres, *Acta Crystallogr., Sect. B: Struct. Crystallogr. Cryst. Chem.*, 1970, **26**, 906–915.
19 C. H. Macgillavry, H. C. J. Dedecker and L. M. Nijland, *Nature*, 1949, **164**, 448–449.
20 R. Kniep, G. Schafer, H. Engelhardt and I. Boy, *Angew. Chem., Int. Ed.*, 1999, **38**, 3642–3644.
21 R. A. Young, *The Rietveld method*, Oxford University Press, New York, 1995.
22 M. I. Pantyukhina, G. V. Zelyutin, N. N. Batalov and V. P. Obrosov, *Russ. J. Electrochem.*, 2000, **36**, 894–898.
23 R. A. Huggins, *Electrochim. Acta*, 1977, **22**, 773–781.